CHEMISTRY

Tilting a ground-state reactivity landscape by vibrational strong coupling

A. Thomas[1]*, L. Lethuillier-Karl[1]*, K. Nagarajan[1], R. M. A. Vergauwe[1], J. George[1]†, T. Chervy[1]‡, A. Shalabney[2], E. Devaux[1], C. Genet[1], J. Moran[1]§, T. W. Ebbesen[1]§

Many chemical methods have been developed to favor a particular product in transformations of compounds that have two or more reactive sites. We explored a different approach to site selectivity using vibrational strong coupling (VSC) between a reactant and the vacuum field of a microfluidic optical cavity. Specifically, we studied the reactivity of a compound bearing two possible silyl bond cleavage sites—Si–C and Si–O, respectively—as a function of VSC of three distinct vibrational modes in the dark. The results show that VSC can indeed tilt the reactivity landscape to favor one product over the other. Thermodynamic parameters reveal the presence of a large activation barrier and substantial changes to the activation entropy, confirming the modified chemical landscape under strong coupling.

Over the years, synthetic chemists have refined the art of designing and developing bond-, site-, and stereoselective chemical reactions using various functional moieties and catalysts. In light of the decisive nature of molecular vibrations in dictating the outcome of isomerization and other chemical processes (*1*–*3*), a physical approach based on the selective excitation of vibrational modes by using strong laser fields has also been explored to impart control on chemical reactivity (*4*–*7*). This laser-induced mode-selective chemistry aimed to steer the system along the reaction coordinate and appeared most straightforward for late barrier reactions (*8*, *9*). The vibrational excitation of the C–H bond of an early barrier reaction inhibited formation of the typical product and modified the branching ratio (*10*), even though such an excitation was predicted to have little influence on the outcome (*11*). An adiabatic transfer of excitation to the product stretching mode was also observed when the localized spectator mode of the reactant was pumped in the former experiments, further indicating the complexities of the reactive landscape (*10*, *12*). Although such mode-selective chemistry works well in the gas phase at cryogenic temperatures, intramolecular vibrational energy redistribution (IVR) limits its use for reactions in solution involving large molecules. To overcome such challenges, we started exploring an alternative approach in which the vibrational transition of a molecule is selectively hybridized with the vacuum electromagnetic field of a cavity by means of vibrational strong coupling (VSC) (*13*–*16*). In other words, even in the dark, the zero-point energy fluctuations of the cavity mode can interact with the vibrational transition and lead to the formation of two new vibropolaritonic states (Fig. 1A, P+ and P–) that should affect the Morse potential. We predicted that this splitting could lead to changes in chemical reactivity (*17*) and demonstrated that the rate of silyl cleavage in 1-phenyl-2-trime-thylsilylacetylene is reduced through VSC of the Si–C stretching vibration (*18*). The reaction mechanism was also modified.

Changing the ground-state reactivity landscape under such a weak-field perturbation suggests that VSC could also be used to modify site selectivity. In a proof-of-principle study, we demonstrate that it is indeed possible to tilt the chemical landscape of a reactant to favor one product over another.

To explore the above possibilities, we synthesized the silane derivative, *tert*-butyldimethyl{[4-(trimethylsilyl)but-3-yn-1-yl]oxy}silane (called **R** hereafter) (Fig. 1B), which incorporates two distinct sites for prospective silyl bond cleavage (supplementary materials) (*19*, *20*). Nucleophilic attack by a fluoride ion on either Si atom can result in the respective cleavage of the Si–C bond, yielding product **1**, or the Si–O bond, yielding product **2** (Fig. 1B). Because both products form through similar mechanistic pathways, we explored first whether the selective strong coupling of vibrational modes respectively associated with Si–C and Si–O has similar or different influences on the reactivity. The second and most important point of the present study was to ascertain whether changes in the reactivity landscape under VSC lead to site selectivity and thereby changes to the branching ratio of the products as schematically presented in Fig. 1, B and C.

Light-matter hybridization is generally achieved by placing molecules in the liquid or solid phase into a Fabry-Perot optical cavity with a mode tuned in resonance with the chosen molecular transition (*21*). When the exchange of energy between the molecular transition and cavity mode is faster than any decay process, the system is said to be in a strong coupling regime manifested by the splitting of the molecular transition into two new states separated by a Rabi splitting energy, $\hbar\Omega_R$ (where $\hbar$ is Planck's constant h divided by 2π and Ω_R is the Rabi frequency), as shown schematically in Fig. 1A with VSC as a specific example. Strong coupling strength and therefore the Rabi splitting increases as the square root of the concentration of coupled molecules (*21*). Under such collective strong coupling conditions, the Rabi splitting can be so large that it results in substantial modification of characteristic properties beyond chemical reactivity, such as electrical conductivity (*22*), rates of energy transfer (*23*, *24*), and reverse intersystem crossing (*25*). This has led to many experimental and theoretical studies of strongly coupled molecular systems [for example, (*26*–*38*)]. For those not familiar with light-matter strong coupling, it might be understood through analogy with the concept of a charge transfer complex. Whereas electrons are shared between two moieties in a charge transfer complex, in light-matter strong coupling, photons are shared between the cavity and the molecules. Although it is well established that in the first case, chemical properties change, we demonstrate again that this is also the case for strong coupling. A detailed introductory explanation of strong coupling of molecules is available in (*21*).

The Fabry-Pérot cavity used in the present experiments comprised two parallel metal mirrors (Au-coated ZnSe) separated by Mylar spacers of different thicknesses (6 to 8 μm), with a hollow central channel designed to inject liquid samples (*15*). To ensure that the reaction dynamics were not affected by the presence of Au or ZnSe, an additional 200-nm-thick layer of glass (SiO_2) was deposited on the inner surface of each window. A homogeneous solution of the starting material **R** (0.90 M) and tetrabutylammonium fluoride (TBAF; 0.86 M) in a 1:1 (v/v) mixture of methanol and tetrahydrofuran (THF), optimized for strong coupling conditions by using a high concentration of **R** to achieve the highest Rabi splittings, was used as the reaction medium throughout the experiments presented here. The infrared (IR) spectrum of **R** (Fig. 2A) in this mixture recorded outside the cavity shows the characteristic strong bands corresponding to the Si–C (842 cm^{-1}) and Si–O (1110 cm^{-1}) stretching modes and the bending mode of the CH_3 groups bonded to Si (1250 cm^{-1}).

VSC requires the cavity mode to be in resonance with a specific IR transition of **R**. This was achieved through careful adjustment of the spacer thickness by tightening or loosening the screws holding the assembly together to vary the applied pressure (supplementary materials). Injection of the homogeneous reaction mixture into the flow cell Fabry-Pérot cavity, whose second mode (λ) was precisely tuned to 842 cm^{-1}, resulted in the strong coupling of the Si–C stretching transition (Fig. 2B). The appearance of P+

[1]University of Strasbourg, CNRS, ISIS and icFRC, 8 allée G. Monge, 67000 Strasbourg, France. [2]Braude College, Snunit Street 51, Karmiel 2161002, Israel.
*These authors contributed equally to this work. †Present address: Department of Chemical Sciences, Indian Institute of Science Education and Research Mohali, Mohali, India. ‡Present address: Institute for Quantum Electronics, ETH Zürich, CH-8093 Zürich, Switzerland.
§Corresponding author. Email: ebbesen@unistra.fr (T.W.E.); moran@unistra.fr (J.M.)

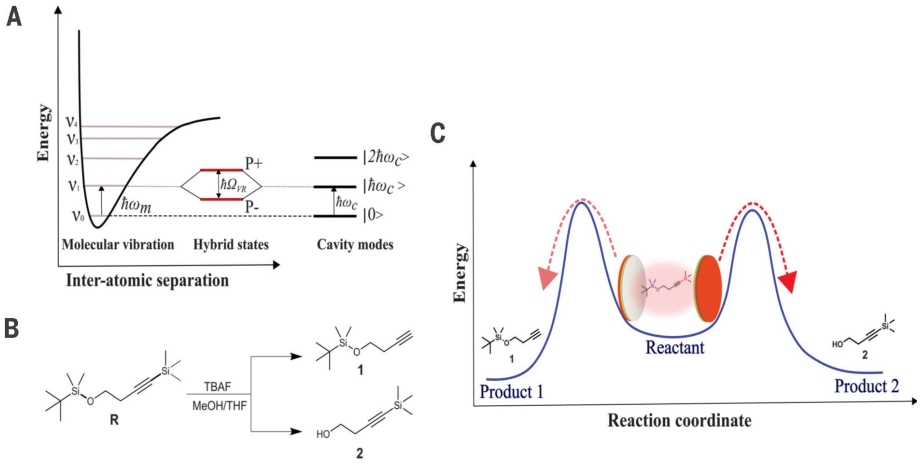

Fig. 1. Test reaction to probe the influence of VSC on site selectivity. (**A**) Schematic illustration of the light-matter strong coupling of a vibrational transition in resonance with Fabry-Pérot cavity mode and the subsequent formation of hybrid polaritonic states P+ and P− separated by Rabi splitting energy, $\hbar\Omega_R$. (**B**) The two major silyl cleavage pathways (Si–C scission to form **1**, Si–O scission to form **2**) for the reaction of **R** with TBAF in a room-temperature mixture of methanol and THF. (**C**) Schematic representation of competing site-selective pathways upon VSC of the reactant.

and P− peaks in the IR spectrum with a $\hbar\Omega_R$ of 70 cm^{-1}, larger than the width of the cavity mode (30 cm^{-1}) and the Si–C vibrational band (30 cm^{-1}), showed that the system meets the strong coupling criteria (*21*). Under these conditions, we also observed a largely detuned coupling between the bending mode of the CH_3 groups bonded to Si (Si–CH_3; 1250 cm^{-1}) and the third mode of the cavity. The influence of the strongly coupled Si–CH_3 bending vibration on the reactivity was analyzed separately and is described later. In a different experiment, VSC of the Si–O stretching band was achieved by tuning the third mode of the cavity to 1110 cm^{-1} (Fig. 2C, solid line). The presence of the intense and broad vibrational modes of the solvents (1040 to 1060 cm^{-1}) splits and reduces the P− band intensity (Fig. 2C) and complicates the spectrum analysis. Therefore, we calculated the $\hbar\Omega_R$ in this case using the standard optics technique (transfer matrix simulation, as explained in the supplementary materials) (Fig. 2C, dotted line). The extracted value of 85 cm^{-1} is well above the cavity and IR mode widths.

The sum rates of the two parallel silyl cleavage reactions under the influence of VSC were quantitatively determined from the ln plot of the temporal shift of a higher-order cavity mode (from $\bar{\nu}_0$ to $\bar{\nu}_t$) (supplementary materials). Similar to the earlier experiment (*18*), this analysis was aided by the slight change in the refractive indices of the reactant and products. The linearity of the ln plot (Fig. 2E) supported first-order kinetics, and from the slope, the rate constant corresponding to the disappearance of starting material was determined. The observed first-order kinetics for this bimolecular reaction is an indication of a complex reaction mechanism, as documented in the literature (*39*, *40*). When the Si–C stretching bond vibration was strongly coupled, the rate was retarded (Fig. 2E, red diamond) by a factor of 3.5 ± 0.2 compared with the control measurements done outside the cavity (Fig. 2E, blue triangle) or inside the cavity under off-resonance conditions (Fig. 2E, green square), when the cavity was not tuned to any of the selected vibrational transitions of **R**. Similarly, strong coupling to the Si–O stretch to the cavity slowed the overall rate by a factor of 2.5 ± 0.1 relative to the outside cavity/off resonant conditions (Fig. 2E, orange circle). The error margin was determined from the standard deviation of a minimum of five experiments.

The reaction mixtures were quantitatively analyzed by means of gas chromatography–mass spectrometry (GC-MS) after each experiment (supplementary materials). The presence of unreacted starting material (labeled **R** in fig. S9) in all the chromatograms showed that the reaction was far from completion in the 3-hour time period and that the ratio did not change over time within the limits of the experiments. The ratios ([**1**]/[**2**]) of the Si–C cleavage to Si–O cleavage product concentrations were further quantified from the GC-MS. For outside cavity and off-resonance reactions, the ratios favored Si–C cleavage and were equivalent within experimental error (1.5 ± 0.2 and 1.4 ± 0.1, respectively). A remarkable increase in the peak area of product **2** was seen when the Si–C stretching vibration was strongly coupled (Fig. 2F, red chromatogram), with a modified branching ratio [**1**]:[**2**] of 0.3 ± 0.1. This value takes into account the fraction of the Fabry-Perot microfluidic cavity under strong coupling. As explained in the supplementary materials, ~60% of the cavity is under VSC because of the deformation of the mirrors when the cavity is tuned by applying pressure with screws. The remaining 40% is detuned beyond the width of the vibrational mode and, as a consequence, is in the off-resonance condition. At the same time, the reaction rate is monitored through a small aperture in the central tuned area. A higher product ratio (0.4 ± 0.1) was observed when the Si–O stretching vibration was strongly coupled. Thus, VSC of the stretch vibration at either site modifies the reactive landscape in favor of Si–O cleavage over the otherwise kinetically favored Si–C cleavage.

As discussed earlier, previous mode-selective chemistry experiments have shown that spectator modes—vibrations that are not directly linked to the reaction coordinate—also play a critical role in determining reaction outcomes (*10*, *41*). In the present case, the strong IR band at 1250 cm^{-1}, arising from the bending mode of the $^{-}CH_3$ groups bonded to Si (*42*), can be considered a spectator vibration. However, the appearance of this IR transition at 1250 cm^{-1}, which one would normally expect at ~1460 cm^{-1} if it is an isolated $^{-}CH_3$ group, already indicates that it is interacting with other vibrations associated with the Si center. By varying the spacer thickness, we achieved VSC of this bending mode alone (Fig. 2D) with a $\hbar\Omega_R$ of 43 cm^{-1}, without simultaneously coupling either the Si–C or Si–O stretching vibrations. VSC of the 1250 cm^{-1} vibration reduced the overall reaction rate by a factor of 3.5 ±0.1 (Fig. 2E, magenta triangle), which is in close similarity to the results obtained under VSC of the Si–C stretching transition and gave rise to a product ratio [**1**]/[**2**] of 0.3 ± 0.1 (Fig. 2F, magenta chromatogram). The question then arises whether the VSC of any vibrational mode of **R** would lead to similar results or whether the effects are restricted to those vibrations that are associated with the reactive Si centers. To explore this question, we coupled the cavity to the C–O stretching transition (at 1045 cm^{-1}) of **R**, a vibration that should have little influence on the reaction from a mechanistic point of view. This mode is also embedded in the broad region (1040 to 1060 cm^{-1}) (Fig. 2A) corresponding to the C–O vibrations of the solvents used (methanol and THF) and so should also serve as a probe of whether coupling to a solvent vibration influences the outcome of the reaction. We observed that neither the rate nor the product ratio was affected by VSC of this C–O transition (fig. S10).

We completed these experiments by measuring the overall observed reaction rate (k_{obs}) as a function of cavity tuning across the IR spectrum of **R** to obtain an action spectrum (Fig. 3A) that clearly confirms which vibrational modes influence the reaction under VSC. This plot reflects the precise selectivity that can be achieved by this weak-field physical perturbation tool at room temperature. Tuning the cavity so that VSC occurs at normal incidence is essential to observe the modification of chemical properties. In this condition, the system is at the minimum energy in the polaritonic state.

By combining the observed overall rate constant (k_{obs}) of the parallel reaction and the product ratios ([**1**]/[**2**]) from GC-MS measurements, we estimated the individual rate constants corresponding to the Si–C (k_1) and Si–O (k_2) bond scissions. From the data, the respective product

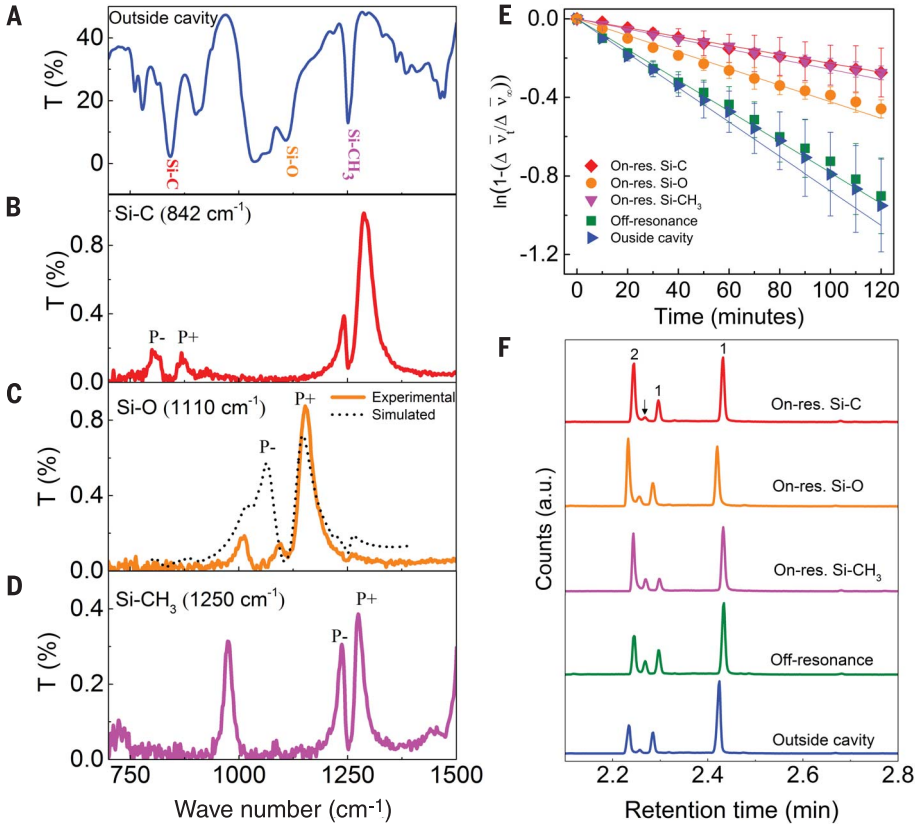

Fig. 2. VSC spectra and relative bond scission kinetics. (**A**) Fourier transform IR (FTIR) transmission spectrum of the starting material **R** in the reaction mixture recorded in a sample cell, with glass-coated ZnSe windows separated by the same spacer thickness as of the Fabry-Pérot cavity. (**B** to **D**) FTIR transmission spectra showing P+ and P– splitting when the three different modes are strongly coupled to the cavity. (B) The Si–C stretching mode. (C) The Si–O stretching mode together with a transfer matrix simulated transmission spectrum (black dotted line). (D) Si–CH_3 bending vibration. (**E**) Kinetics of the reactions in cavities tuned to be on-resonance with the Si–C stretching (red diamonds), the Si–O stretching (orange circles), and the Si–CH_3 bending modes (magenta triangles), together with the data for an off-resonance cavity (green squares) and outside the cavity (blue triangles), as extracted from the temporal shifts in the higher-order cavity modes. The error bars show the standard deviations for a minimum of five independent experiments for each case. (**F**) The GC-MS chromatograms of the reactions carried out in cavities tuned to be on-resonance with Si–C stretching (red), Si–O stretching (orange), and Si–CH_3 bending modes (magenta), together with the data for an off-resonance cavity (green) and outside the cavity (blue). The peaks corresponding to C- and O-deprotected products are marked as **1** and **2**, respectively. The peak indicated by the arrow is an impurity that comes from the slow degradation of the GC-MS column and is present in all the chromatograms that we measured. These chromatograms are zoomed in on the products for clarity; the complete ones can be found in fig. S9.

yields were calculated. The yields (ϕ) of products **1** and **2** in and out of strong coupling for various coupling conditions are shown in Fig. 3B. Outside the cavity and in off-resonance conditions, the k_1 dominates over k_2, resulting in preferential formation of product **1** (Fig. 3B, purple diamond). VSC reverses the selectivity, leading to an excess formation of product **2** (Fig. 3B, pink squares). This is again a direct proof of principle that the chemical landscape can be tilted by targeting the three vibrational modes associated with the reaction centers. The values of both k_1 and k_2 under strong coupling conditions are lower than those observed outside the cavity, indicating that a higher activation energy is required for the reaction under VSC. Products **1** and **2** undergo further silyl bond cleavage, although the subsequent reactions appear to be much slower, resulting in the accumulation of **1** and **2** in the GC-MS analysis. These downstream reactions impart a small error in the yields but have no consequence on the overall results.

The thermodynamics of the two bond-breaking reactions that lead to products **1** and **2** were determined by measuring the rates as a function of temperature under VSC of the Si–C and Si–O stretching vibrations as well as outside the cavity. Using transition state theory, the free energy of activation ($\Delta H^{\ddagger}$) and the entropy of activation ($\Delta S^{\ddagger}$) were determined from the slope and intercept of the plot of ln(k) against the inverse of temperature (Fig. 4). The results extracted from the plots of Fig. 4 are summarized in Table 1. It shows that the thermodynamic parameters are substantially changed under VSC for both products but lead to different values for products **1** and **2**. What is surprising is that the new values of $\Delta H^{\ddagger}$ and $\Delta S^{\ddagger}$ appear to be similar whether one couples the Si–C or the Si–O stretching vibrations. This might be fortuitous for the specific molecule under study. It has been shown that the presence of leaving groups far away can change desilylation rates (*43*).

The above results show that VSC can modify the chemical landscape, and the associated $\Delta H^{\ddagger}$

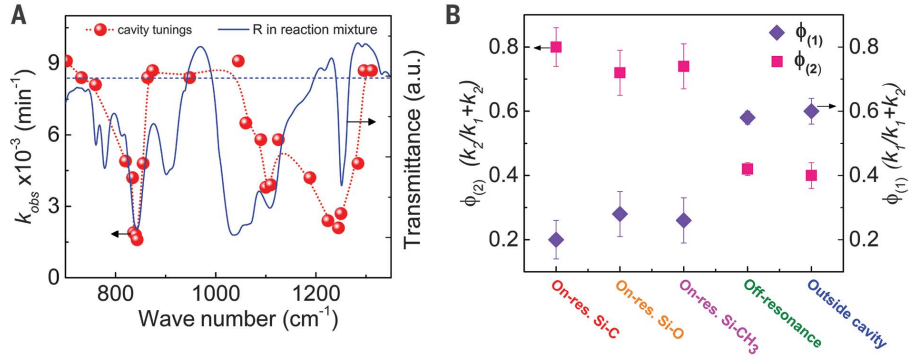

Fig. 3. Relative VSC influence across the vibrational spectrum. (**A**) The overall reaction rate as a function of cavity tuning for reactions inside the cavity (red spheres). The blue solid line shows the IR absorption spectrum of **R** in the reaction medium. The red dotted line connecting the spheres is a guide for the eye. The blue dashed line represents the average rate of the reaction outside the cavity. (**B**) Plot showing the yields of product **1** (ϕ_1; violet diamonds) and **2** (ϕ_2; pink squares) under VSC of various vibrational modes of **R**, together with the off-resonance and outside cavity conditions. The error margin was determined from the standard deviation of a minimum of five experiments in each case.

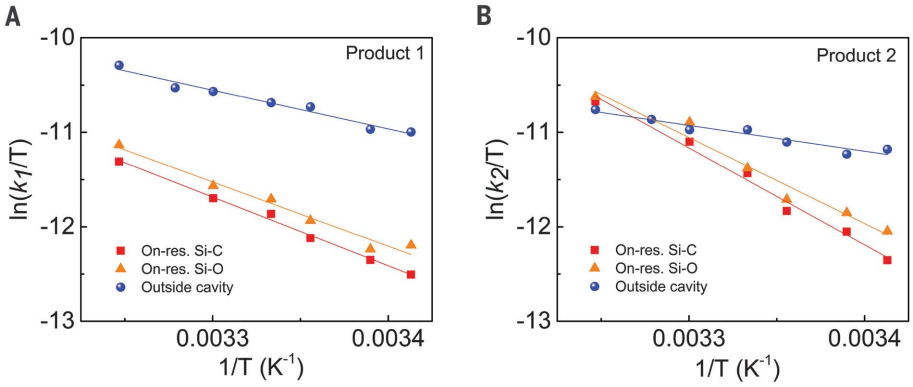

Fig. 4. Eyring plots showing the reaction rate for the formation of products as a function of temperature between 20° and 35°C. (**A**) Formation of product **1**. (**B**) Formation of product **2.** Reactions inside the cavities tuned to be on-resonance with Si–C (red squares) or Si–O (orange triangles) stretching modes are compared with reactions outside the cavity (blue spheres). The data were fitted with a least-square method, and the quality of the fit can be assessed from coefficient of determination (R^2) values ≥0.95.

Table 1. Enthalpy and entropy of activation under strong coupling.

Products	Experiment	$\Delta H^{\ddagger}$ (kJ mol^{-1})	$\Delta S^{\ddagger}$ (J mol^{-1} K^{-1})
Product **1**	Outside cavity	34 ± 3	−173 ± 11
	On-resonance Si–C	60 ± 2	−95 ± 7
	On-resonance Si–O	57 ± 5	−106 ± 17
Product **2**	Outside cavity	23 ± 3	−214 ± 8
	On-resonance Si–C	85 ± 5	−6 ± 17
	On-resonance Si–O	76 ± 7	−39 ± 24

and $\Delta S^{\ddagger}$, in such a way that it tilts the landscape from one product to another. An interesting aspect of chemical reactions under VSC so far has been the high activation barrier seen toward the breaking of Si–C and Si–O bonds. Because a typical fluoride-induced silyl cleavage is known to proceed through an associative mechanism involving a pentacoordinate intermediate (*39*), a strained transition state with large negative $\Delta S^{\ddagger}$ is expected as observed outside the cavity. The observed sharp decrease of $\Delta S^{\ddagger}$ to a lower value under VSC implies that the transition state is strongly modified, particularly the one leading to product **2**. The high activation energy and the less negative $\Delta S^{\ddagger}$ clearly indicate that the reaction switched to a dissociative mechanism under VSC and also suggest that the transition state is product-like, as in the case of late barrier reactions. One potential explanation for the apparent change in mechanism is that VSC suppresses typical associative pathways for Si–C and Si–O bond cleavage, allowing otherwise slower dissociative pathways to dominate. The stronger change under VSC for the dissociative pathway leading to **2** compared with that leading to **1** could therefore be rationalized because the former involves a better leaving group.

Barrier increases have also been seen in earlier experiments, whether occurring in the ground state (*18*) or via the excited state under electronic strong coupling, such as in the photoisomerization reaction of merocyanine (*17*). For the latter case, recent theoretical studies show that the collective response of molecules plays a role in widening the barrier at the conical intersection, preventing the isomerization (*31*, *32*). However, such findings cannot yet be generalized; a recent study of hydrolysis reactions under VSC shows large rate accelerations (up to 10^4) (*44*). More experimental and theoretical studies are required to be able to extract general features and understand the effects of VSC on different types of reactions.

This proof-of-principle study shows that it is possible to control reaction selectivity through VSC. Strong coupling is dependent on the orientation of the transition dipole moment relative to the electric field of the cavity mode. The molecules were randomly oriented, and the electric field was not uniform in the cavity; there were nodes where the field was essentially null. Hence, the fivefold increase in selectivity under VSC reported here is probably much larger if corrected for such features. For instance, experiments could be done in a tubular cavity to ensure a larger fraction of coupled molecules. Therefore, the selectivity displayed by VSC in the current experiment shows the remarkable potential of light-matter strong coupling for enhancing site selectivity of organic and inorganic chemical reactions. More reactions must be studied to evaluate the generality of this phenomenon and to see to what extent the selectivity can be enhanced at a given site. As more and more studies show, this weak-field room-temperature method has the potential to become an everyday tool for chemists to physically control chemical reactivity without catalysts, prefunctionalization, or chemical changes to the reaction conditions.

REFERENCES AND NOTES

1. R. T. Hall, G. C. Pimentel, *J. Chem. Phys.* **38**, 1889–1897 (1963).
2. Q. Wang, R. W. Schoenlein, L. A. Peteanu, R. A. Mathies, C. V. Shank, *Science* **266**, 422–424 (1994).
3. M. Delor *et al.*, *Science* **346**, 1492–1495 (2014).
4. H. Frei, L. Fredin, G. C. Pimentel, *J. Chem. Phys.* **74**, 397–411 (1981).
5. A. Sinha, M. C. Hsiao, F. F. Crim, *J. Chem. Phys.* **94**, 4928–4935 (1991).
6. R. N. Zare, *Science* **279**, 1875–1879 (1998).
7. F. F. Crim, *Acc. Chem. Res.* **32**, 877–884 (1999).
8. S. Yan, Y.-T. Wu, B. Zhang, X.-F. Yue, K. Liu, *Science* **316**, 1723–1726 (2007).
9. D. R. Killelea, V. L. Campbell, N. S. Shuman, A. L. Utz, *Science* **319**, 790–793 (2008).
10. W. Zhang, H. Kawamata, K. Liu, *Science* **325**, 303–306 (2009).
11. J. C. Polanyi, *Acc. Chem. Res.* **5**, 161–168 (1972).
12. K. Liu, *Annu. Rev. Phys. Chem.* **67**, 91–111 (2016).
13. A. Shalabney *et al.*, *Nat. Commun.* **6**, 5981 (2015).
14. J. P. Long, B. S. Simpkins, *ACS Photonics* **2**, 130–136 (2015).
15. J. George *et al.*, *Phys. Rev. Lett.* **117**, 153601 (2016).
16. R. M. A. Vergauwe *et al.*, *J. Phys. Chem. Lett.* **7**, 4159–4164 (2016).
17. J. A. Hutchison, T. Schwartz, C. Genet, E. Devaux, T. W. Ebbesen, *Angew. Chem. Int. Ed.* **51**, 1592–1596 (2012).
18. A. Thomas *et al.*, *Angew. Chem. Int. Ed.* **55**, 11462–11466 (2016).
19. R. J. Rahaim Jr., J. T. Shaw, *J. Org. Chem.* **73**, 2912–2915 (2008).
20. S. V. Shelke *et al.*, *Angew. Chem. Int. Ed.* **49**, 5721–5725 (2010).
21. T. W. Ebbesen, *Acc. Chem. Res.* **49**, 2403–2412 (2016).
22. E. Orgiu *et al.*, *Nat. Mater.* **14**, 1123–1129 (2015).
23. X. Zhong *et al.*, *Angew. Chem. Int. Ed.* **56**, 9034–9038 (2017).
24. C. Gonzalez-Ballestero, J. Feist, E. Moreno, F. J. Garcia-Vidal, *Phys. Rev. B* **92**, 121402 (2015).
25. K. Stranius, M. Hertzog, K. Börjesson, *Nat. Commun.* **9**, 2273 (2018).
26. S. Wang *et al.*, *J. Phys. Chem. Lett.* **5**, 1433–1439 (2014).
27. S. Gambino *et al.*, *ACS Photonics* **1**, 1042–1048 (2014).
28. W. Ahn, I. Vurgaftman, A. D. Dunkelberger, J. C. Owrutsky, B. S. Simpkins, *ACS Photonics* **5**, 158–166 (2018).
29. M. Hertzog *et al.*, *Chemistry* **23**, 18166–18170 (2017).
30. O. Kapon, R. Yitzhari, A. Palatnik, Y. R. Tischler, *J. Phys. Chem. C* **121**, 18845–18853 (2017).
31. J. Galego, F. J. Garcia-Vidal, J. Feist, *Nat. Commun.* **7**, 13841 (2016).
32. J. Galego, F. J. Garcia-Vidal, J. Feist, *Phys. Rev. Lett.* **119**, 136001 (2017).
33. V. F. Crum, S. R. Casey, J. R. Sparks, *Phys. Chem. Chem. Phys.* **20**, 850–857 (2018).
34. G. G. Rozenman, K. Akulov, A. Golombek, T. Schwartz, *ACS Photonics* **5**, 105–110 (2018).
35. D. G. Baranov, M. Wersäll, J. Cuadra, T. J. Antosiewicz, T. Shegai, *ACS Photonics* **5**, 24–42 (2018).
36. F. Herrera, F. C. Spano, *Phys. Rev. Lett.* **116**, 238301 (2016).
37. L. A. Martínez-Martínez, R. F. Ribeiro, J. Campos-González-Angulo, J. Yuen-Zhou, *ACS Photonics* **5**, 167–176 (2018).
38. J. Flick, C. Schäfer, M. Ruggenthaler, H. Appel, A. Rubio, *ACS Photonics* **5**, 992–1005 (2018).
39. A. R. Bassindale, P. G. Taylor, in *Organic Silicon Compounds* (Wiley-Blackwell, 2004), ch.13, pp. 839–892.
40. A. M. DiLauro, W. Seo, S. T. Phillips, *J. Org. Chem.* **76**, 7352–7358 (2011).
41. G. C. Schatz, M. C. Colton, J. L. Grant, *J. Phys. Chem.* **88**, 2971–2977 (1984).
42. A. Grill, D. A. Neumayer, *J. Appl. Phys.* **94**, 6697–6707 (2003).
43. P. M. F. M. Bastiaansen, R. V. A. Orru, J. B. P. A. Wijnberg, A. de Groot, *J. Org. Chem.* **60**, 6154–6158 (1995).

44. H. Hiura, A. Shalabney, J. George, *ChemRxiv* 10.26434/chemrxiv.7234721.v2 (2018).

ACKNOWLEDGMENTS

Funding: We acknowledge support of the International Center for Frontier Research in Chemistry (icFRC, Strasbourg), the ANR Equipex Union (ANR-10-EQPX-52-01), the Labex NIE projects (ANR-11-LABX-0058 NIE), and CSC (ANR-10-LABX- 0026 CSC) within the Investissement d'Avenir program ANR-10-IDEX-0002-02. T.W.E. and J.M. both acknowledge the support of the ERC (project 788482 MOLUSC and 639170 CarbonFix, respectively). **Author contributions:** A.T. and L.L.-K. took the lead in all the experiments, assisted by K.N., R.M.A.V., J.G., T.C., A.S., and E.D.; C.G. provided theoretical insight, and J.M. and T.W.E. conceived and oversaw the experiments. **Competing interests**: The authors declare no competing interests. **Data and materials availability:** All data are available in the main text or the supplementary materials.

SUPPLEMENTARY MATERIALS

www.sciencemag.org/content/363/6427/615/suppl/DC1
Materials and Methods
Figs. S1 to S10
Table S1
Reference (*45*)

13 July 2018; accepted 8 January 2019
10.1126/science.aau7742

Tilting a ground-state reactivity landscape by vibrational strong coupling

A. Thomas, L. Lethuillier-Karl, K. Nagarajan, R. M. A. Vergauwe, J. George, T. Chervy, A. Shalabney, E. Devaux, C. Genet, J. Moran and T. W. Ebbesen

Science **363** (6427), 615-619.
DOI: 10.1126/science.aau7742

Shaking up reaction-site selectivity

It seems intuitive that putting vibrational energy into a chemical bond ought to promote selective cleavage of that bond. In fact, the relation of vibrational excitation to reactivity has generally proven subtler and more complex. Thomas *et al.* studied how strong coupling of specific vibrational modes to an optical cavity might influence a molecule with two competing reactive sites. The molecule had two silicon centers that could react with fluoride by respective cleavage of a Si–C or Si–O bond. Exciting the vibrations at either center slowed down the overall reaction while favoring otherwise disfavored Si–O cleavage.

Science, this issue p. 615